# A kinetic theory model of human crowds accounting for visual attention

**Jun Ma, Meiling Wang and Linze Li**

## Abstract

The visual attention of pedestrians has been rarely considered in studies of congestion prevention in long-distance passages. This paper proposes a kinetic theory model of human crowds accounting for visual attention to study congestion in long-distance passages. The population is divided into visual attention-shifting pedestrians (VAS pedestrians) and nonvisual attention-shifting pedestrians (non-VAS pedestrians). First, the movement characteristics of all pedestrians are analyzed based on observations and measurements obtained through controlled experiments. Moreover, a pedestrian flow model accounting for visual attention is built to transform the characteristics of pedestrian movement into a mathematical model. Finally, validation is done, and the density and the proportion of VAS pedestrians are selected as congestion warning parameters. Simulations are performed for a subway passage connected to stairs, and the effect of visual attention, the critical thresholds of congestion warning parameters, and the effects of implementing mitigation measures immediately after congestion occurs are assessed. The experimental results show that the movement characteristics of VAS pedestrians and non-VAS pedestrians are different. Simulation results show that the model is effective. Notably, visual attention has an impact on pedestrian movement, and using the density and the proportion of VAS pedestrians as early warning indicators is effective for preventing the occurrence of congestion, as demonstrated by the negative correlation between the two critical thresholds. This description of human groups provides quantitative guidelines for crowd management.

## 1. Introduction

Visual attention shift is a common behavior in daily life, but it can result in the occurrence of accidents. According to previous research, approximately 25% of car accidents are caused by driver inattention and this rate is gradually increasing with the development of smartphones.[1] Accidents also may occur among pedestrians. Visual attention shift slows pedestrian walking speeds in narrow and long passages (as shown in Figure 1), which may lead to stampedes and congestion. The frequent occurrence of safety incidents caused by congestion increases the travel time cost of pedestrians and can even lead to the loss of life and property, thus making safety management complex and important. Therefore, determining how to control congestion considering visual attention-shifting behavior in long-distance passages is an urgent problem.

Congestion is quite common and has attracted the attention of many researchers. Specifically, the impacts of different factors, including the locations of exits,[2] the internal layout of the system,[3] short-range collision

avoidance,[4] pedestrian age,[5] an imbalanced initial layout of pedestrians,[6] and the kinship effect,[7] on congestion evacuation have been explored. However, these studies did not consider the impact of pedestrians' visual attention-shifting behavior on congestion. Zhao et al.[8] showed that looking down at your phone, a form of visual attention-shifting behavior, leads to longer street crossings. A study in the field of vehicle traffic, similar to the field of pedestrian transportation, reached the analogous conclusion that distracting behavior lengthens the time it takes to cross the street. According to wave theory,[9] the disturbance caused by a decrease in the speed of individuals in dense crowds

School of Management and Engineering, Capital University of Economics and Business, China

**Corresponding author:**
Meiling Wang, School of Management and Engineering, Capital University of Economics and Business, 121 Zhangjia Road Intersection, Fengtai District, Beijing 100070, China.
Email: wangmeiling@cueb.edu.cn
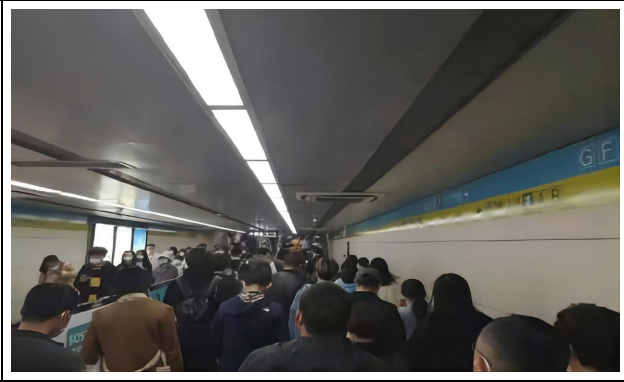
**Figure 1.** Daily scenario involving pedestrians' visual attention-shifting behavior in a long-distance passage.

may lead to the occurrence of congestion accidents. Therefore, it is necessary to consider pedestrian visual attention-shifting behavior in studies of congestion.

In congestion research, a suitable mathematical model that can effectively consider the heterogeneity of visual attention behavior must be selected. According to the research scale, dynamic crowd models can be divided into three types: microscale models,[10–16] macroscale models,[17–23] and mesoscale models (kinetic models).[24–32] Microscale models are used to analyze and model individual motion characteristics and they include the social force model and the cellular automaton model. The social force model originated from Lewin's domain theory[10] and was developed based on Helbing's introduction of Newton's mechanical concept. This model is a continuous model for pedestrian flow movement associated with the superposition of self-driving forces, exclusion forces, attraction, and other social forces.[11] The cell automaton model considers a crowd to be composed of discrete cells that evolve in discrete time and space according to certain movement rules.[12] These models can satisfy the behavioral heterogeneity of constraints related to the visual attention state of pedestrians, but many equations and iterations may be required to obtain a solution, leading to a high calculation cost. Macroscale models are based on the mechanical assumption of continuous media and the microscopic interactions between pedestrians are ignored; thus, the features of pedestrian flows are assessed from a global perspective. The most common models are hydrodynamic models. Hughes assumed that pedestrian flow is a compressible continuous fluid and derived the corresponding two-dimensional pedestrian flow motion equation based on the continuity equation.[17,18] A macroscale model cannot describe heterogeneous pedestrian movement because in the derivation process, the parameters related to heterogeneity are averaged. Moreover, a macroscale model assumes that a crowd is completely continuous, but in reality, even high-density pedestrian flows have spatial gaps; therefore, these flows should be modeled as incomplete continuous fluids because of the heterogeneity of individual walking strategies.

Microscale and macroscale models are not suitable for use in dynamic crowd modeling in this study, but mesoscale models can overcome the limitations of these models. Mesoscale models are used for the analysis and modeling of local groups and they include particle models based on kinetic theory. Based on kinetic theory for active particles, Bellomo and colleagues used stochastic game theory to describe the interactions of pedestrians and used the balance among the number of particles associated with different microelements to establish a suitable model of pedestrian movement.[24–29] A mesoscale model can reflect the random uncertainty of crowd movement based on the relationship between individual motion characteristics at the microscale and upstream pedestrian flow parameters at the macroscale. Therefore, heterogeneous requirements can be taken into account through considering random uncertainty. Moreover, mesoscale models have the following advantages. First, such models closely reflect reality by treating a crowd as a multiparticle system. Second, mesoscale models use statistical methods to describe the state of a crowd and model the evolution of the pedestrian speed distribution considering individual interactions; therefore, the closed-loop speed–density relationship does not need to be introduced in advance. Third, mesoscale models are multiscale models that can reveal the inherent trends in crowd dynamics from multiple perspectives and they require few calculations and provide detailed results.

Based on the above advantages, a particle model based on kinetic theory is suitable for solving congestion problems considering visual attention. The first relevant particle model was derived by Bellomo and colleagues[24] and has been adapted to different systems under consideration, such as a space with internal obstacles,[27] panic cases,[26] and evacuation from a complex venue.[33] However, visual attention has not been considered in the studies based on this model.

In addition, appropriate parameters related to congestion risk are also necessary. At present, research on congestion parameters mainly focuses on density. Zhang et al.[34] established a congestion density prediction model based on a Markov chain to determine where abnormal crowds gather in public areas in cities. Bai et al.[35] established a crowd density detection method based on the congestion mode and a multicolumn convolutional neural network to facilitate congestion safety evaluation. Teo et al.[36] proposed a wearable electronic device that helps mitigate such disasters by directing people and thus controlling the density of the crowd. These studies used density and other related quantities as indicators of congestion. However, management measures based on density may reduce the circulation efficiency in channels.

Therefore, it is necessary to add new parameters to traditional models to prevent channel congestion.

In this paper, an active particle model based on kinetic theory is introduced. Specifically, this model is a mesoscale model that can be applied to assess human crowd dynamics considering visual attention, and new congestion indicators are proposed to solve the congestion risk prevention and control problem in long-distance passages. Individuals in a crowd are divided into two types according to their visual attention states: visual attention-shifting pedestrians (VAS pedestrians) and nonvisual attention-shifting pedestrians (non-VAS pedestrians). The main contributions of this work are as follows:

1. The motion characteristics of VAS and non-VAS pedestrians are analyzed in long-distance passages to determine the parameters that should be included in the crowd dynamics model.
2. We propose a kinetic theory model of human crowds considering visual attention to investigate crowd dynamics over long distances. The model converts the motion characteristics of pedestrians into mathematical expressions. In addition, the influence of visual attention on crowd dynamics is investigated.
3. The density and the proportion of VAS pedestrians are selected as warning parameters.

The remainder of this paper is organized as follows. In "Motion characteristics of VAS and non-VAS pedestrians in long-distance passages" section, the motion characteristics of pedestrians are analyzed based on observed and measured data from a long-distance passage. The details of the model are given in "Model description" section. In "Simulations" section, the validity of the model is verified and a scene is simulated to show how to use the above model to prevent and control congestion problems. In addition, warning parameters are selected and their threshold values are tested to provide a numerical basis for managers. In "Conclusion and future work" section, the content of this paper is summarized, and some research prospects are proposed.

## 2. Motion characteristics of VAS and non-VAS pedestrians in long-distance passages

The motion characteristics of pedestrians can provide a reliable and practical basis for selecting the parameters of a model. In this paper, the movement characteristics of VAS and non-VAS pedestrians in long-distance passages are assessed based on controlled experiments. It is important to clarify the definitions of long-distance passages and

shifts in visual attention before analyzing the motion characteristics. The concept of a long-distance passage is defined as follows.

*Definition 2.1.* A long-distance passage is a corridor in which pedestrian motion occurs for at least 10 m. Such corridors include underground pedestrian passages, subway transfer passages, hallways, and so on.

The definition of a shift in visual attention can be formed based on the results of previous vehicle traffic studies. Regan et al.[37] suggested that distraction is a form of negligence for drivers when they shift from an important driving task to a competing behavior. When a driver's focus deviates from the driving task, the driver is considered distracted.[38,39] Therefore, a shift in visual attention is defined as follows.

*Definition 2.2.* A shift in visual attention occurs because of an event-, activity-, object-, or person-related force that causes a shift in attention during walking tasks. In such cases, the information required for pedestrians to safely complete walking tasks is completely or partially ignored.
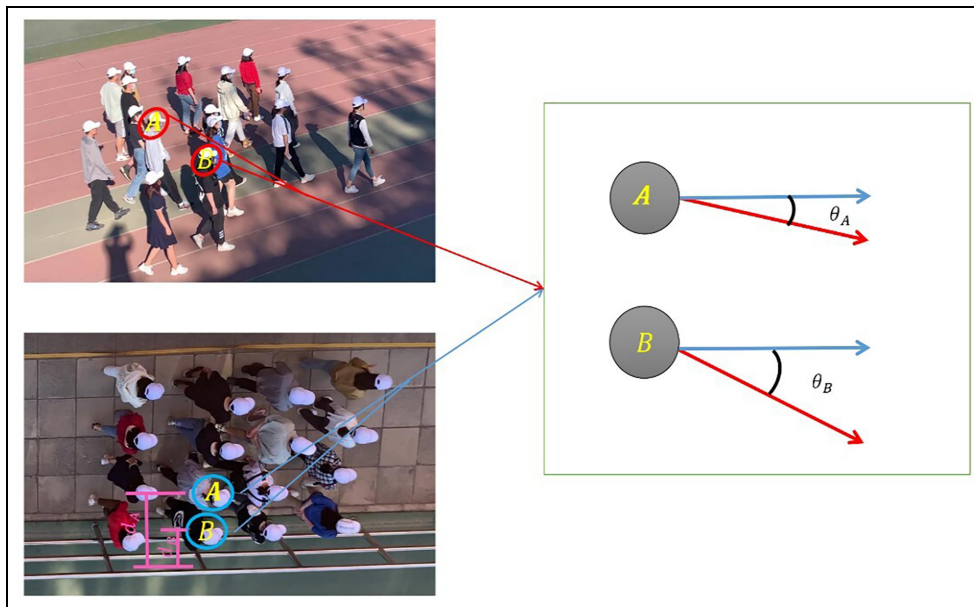
### 2.1. Walking direction

*2.1.1. The influence of boundaries.* Hughes suggested that pedestrians seek to minimize their travel time and avoid high-density areas when formulating walking strategies.[18] However, the movement of pedestrians in long-distance passages, as closed spaces, is influenced by boundaries. Experiments in open space and long-distance passages have been conducted to observe the influence of boundaries. Notably, open space and artificial long-distance passages (10 m $\times$ 2 m) were established. Sixteen volunteers participated in the experiment. Pedestrians wore white hats to facilitate the identification of their respective locations. Initially, pedestrians were required to stand outside the experimental area in a 4 $\times$ 4 formation and the exit was established as a moving target. After the experiment started, pedestrians moved toward the exit. The experimental process is shown in Figure 2.

In the experiments, the pedestrians moved in different directions in the two spaces. Pedestrians in the unbounded space moved toward not only the exit but also toward the low-density areas on both sides of the main crowd. However, in the long passage, pedestrians could not move into low-density areas because of boundary limitations.

Movement direction diagrams of two pedestrians in the different spaces were created for the same point in time ($t = 20$ s) and based on the same initial conditions, as shown in Figure 3. Notably, the closer to the boundary of the long passage a pedestrian is ($d_A > d_B$), the greater the restriction on their walking direction ($\theta_A < \theta_B$).
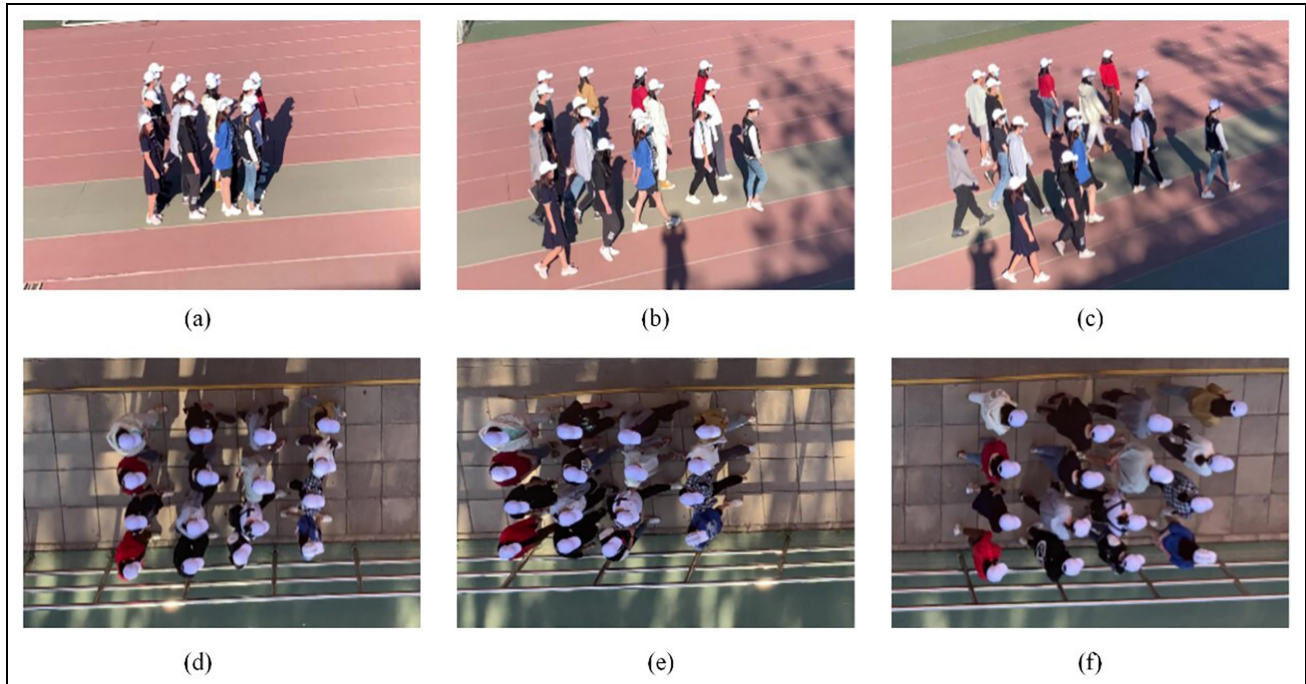
**Figure 2.** Snapshots of the experiments (a, b, c) without and (d, e, f) with boundaries. The images were captured at the following times: (a) $t = 0$ s, (b) $t = 10$ s, (c) $t = 20$ s, (d) $t = 0$ s, (e) $t = 10$ s, and (f) $t = 20$ s.



**Figure 3.** Walking direction diagrams of pedestrians in spaces without and with boundaries after 20 s.

*2.1.2. Walking directions associated with different interaction types.* In a high-density environment, pedestrians in various visual attention states may be affected by other pedestrians in the same or different states. Therefore, some experiments were conducted to observe the walking

direction choices of pedestrians affected by pedestrians in various visual attention states. The experimental scene was set in an artificial long-distance passage (10m × 2m). Fifteen volunteers participated in the experiment. The initial queue used in the experiments is shown in Figure 4. It
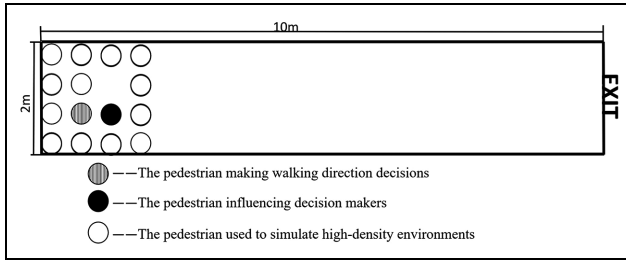
**Figure 4.** Initial pedestrian placements in the walking direction for different interaction types.

is worth noting that there is a space left in front of the pedestrian who makes decisions regarding the walking direction to facilitate the possible overtaking behavior of VAS or non-VAS pedestrians. When the experiment began, pedestrians walked toward the exit and made walking direction decisions according to their individual preferences. The results of the experiments are shown in Figure 5.

Figure 4 shows that regardless of whether the influencer is a non-VAS or VAS pedestrian, the pedestrians making walking direction decisions who are non-VAS pedestrians all adopt transcendence behaviors (Figures 4(a) and 5(b)); in addition, regardless of whether the influencer is a non-VAS or VAS pedestrian, pedestrians making walking direction decisions who are VAS pedestrians all adopt following behaviors (Figure 5(c) and (d)).

In summary, VAS and non-VAS pedestrians choose their walking directions based on specific characteristics. For VAS pedestrians, the walking direction is mainly affected by the exit location, denoted as $V_t$ in Figure 6(a). For non-VAS pedestrians, their movement direction is mainly affected by the walls, the exit location $V_t$, and the minimum density of pedestrians, denoted as $V_\rho$; this movement pattern generally involves two steps. First,
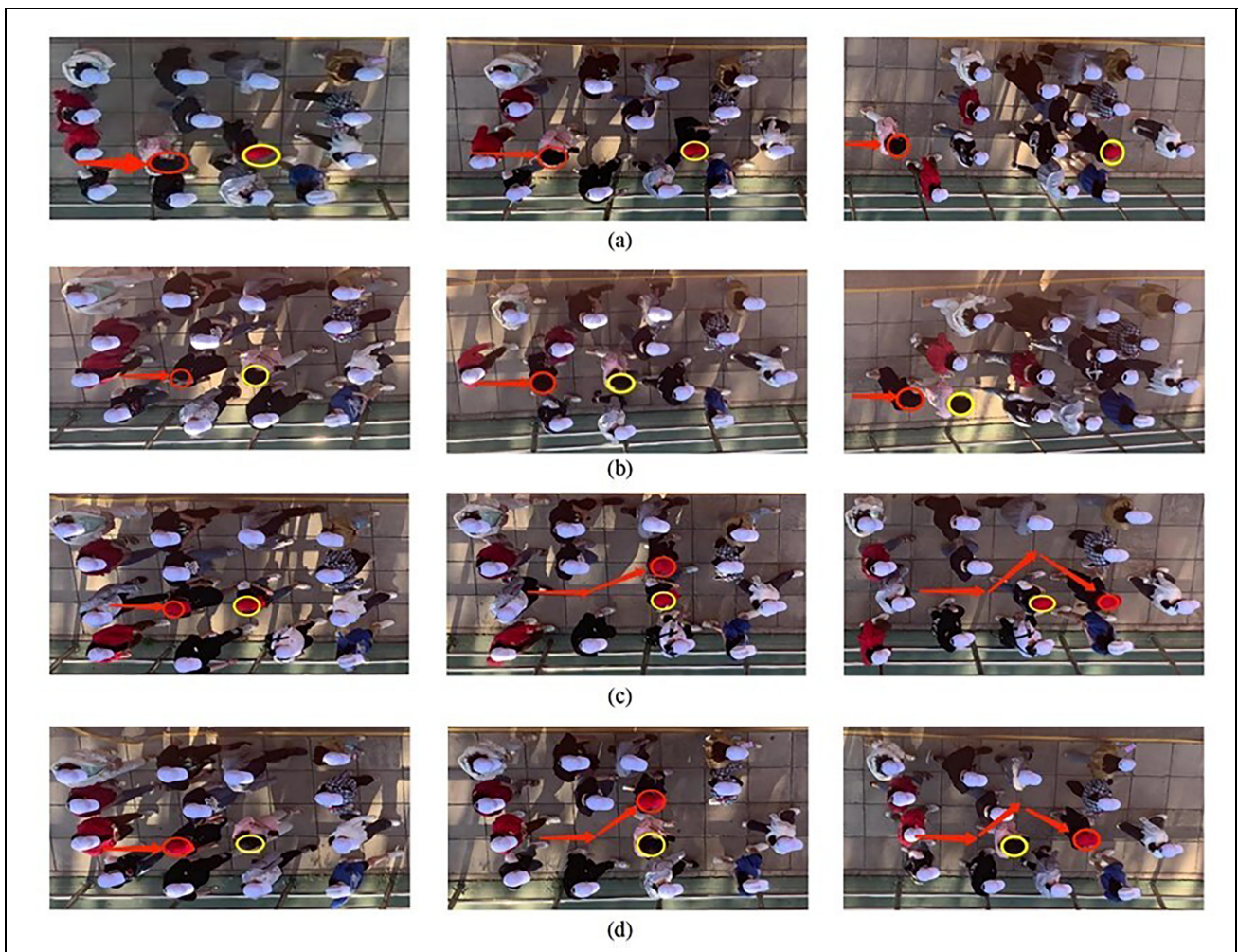


**Figure 5.** Snapshots of walking direction experiments for different interaction types. The scenarios include (a) non-VAS and non-VAS, (b) non-VAS and VAS, (c) VAS and non-VAS, and (d) VAS and VAS interaction types.
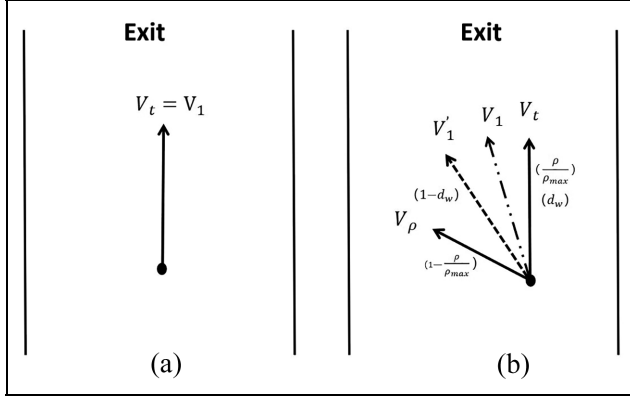
**Figure 6.** Characteristics of VAS and non-VAS pedestrians choosing walking directions. (a) VAS pedestrians are only affected by the exit location $V_t$. (b) Non-VAS pedestrians are affected by the exit location $V_t$, minimum density gradient $V_\rho$, and boundaries. Choosing a walking direction involves two steps. First, the vector sum $V_1'$ of $V_t$ and $V_\rho$ is calculated. The second walking direction $V_1$ is then calculated as the vector sum of $V_1'$ and $V_t$. The expressions in parentheses give the weights of different factors.

pedestrians will walk toward $V_1'$ according to the exit location $V_t$ and the minimum density gradient $V_\rho$, and their degree of influence can be described by the local density $\rho$. If the local pedestrian density $\rho$ is high, non-VAS pedestrians will tend to avoid high-density areas; therefore, $V_\rho > V_t$. In contrast, if the density $\rho$ is low, non-VAS pedestrians will prefer to move toward the exit, that is, $V_\rho < V_t$. Second, if the gradient $V_1'$ points to the boundary, then $V_1'$ needs to be corrected to $V_1$ based on making a weighted choice between $V_1'$ and $V_t$ and this weight is given by the shortest length $d_w$ from the boundary. The farther an individual gets from a boundary, the more that pedestrian will prefer to move toward the exit $V_t$, as shown in Figure 6(b).

## 2.2. Speed

The decision-making process of pedestrians is related in part to speed behavior, including passing behavior and following behavior. When pedestrians rotate in the direction they want to move, they will collect some information about the speed of other pedestrians and general information about their surroundings. Then, an individual assesses the speed relationships between other pedestrians and themselves according to their cognitive state. Finally, they decide whether to adjust their own speed decision. If $v > \bar{v}$, pedestrians are restricted by other people, which leads to slowing down or even stopping. If $v = \bar{v}$, pedestrians will choose to maintain their original speed or decelerate. In addition, if $v < \bar{v}$, pedestrians will choose to maintain their original speed or accelerate. The decision to

change or maintain speed mainly depends on the individual's cognitive state.[29] The cognitive state of each person is different based on the effects of rational consciousness, analytical reasoning ability, recognition and judgment ability, memory ability, and so on. That is, the choice of pedestrians to change or maintain speed is random. If pedestrians choose to change speed, they need to further consider factors related to the speed change. Pedestrian speed changes are determined by their own behavioral choices,[40] the movement state of the surrounding pedestrians,[26] and the ground slope.[41] The influence of these factors on speed will be explored through experiments in this section. It is worth noting that there may be obstacles in the interaction domain that affect pedestrian sight and pedestrians may not necessarily perceive other people's movement information. The specific process is shown in Figure 7.

*2.2.1. VAS deceleration coefficient.* The VAS deceleration coefficient refers to the ratio of the speed of VAS pedestrians to the speed of non-VAS pedestrians, denoted as $\gamma$, and the value range is [0,1]. This variable reflects the speed reduction associated with a shift in visual attention. Experiments were performed in a long horizontal passage to assess the deceleration coefficient of pedestrians. Thirty-two pedestrians, including 16 men and 16 women, participated in the experiment. Each pedestrian was required to walk twice in the passage, with one scenario involving free walking and the other involving walking while looking down at a mobile phone, as shown in Figure 8.

The average speed through the long passage was calculated as the speed of volunteers in different visual attention states. Then, the VAS deceleration coefficient for each person was calculated and plotted into a frequency histogram, as shown in Figure 9. Figure 8 shows that the VAS deceleration coefficient is approximately normally distributed. Hence, the distribution function of the VAS deceleration coefficient is defined as shown in Equation (1):

$$f(\gamma) = \frac{1}{0.07\sqrt{2\pi}} e^{\left(-\frac{(\gamma - 0.63)^2}{0.0098}\right)} \tag{1}$$

where $f(\gamma)$ is the probability density function of the VAS deceleration coefficient.

*2.2.2. Variable speed coefficient.* The variable speed coefficient is a correction to the relative speed between pedestrians and influencers, denoted as $\alpha$. This factor is calculated based on Equation (2):

$$\alpha = \frac{v_{t+\Delta t} - v_t}{\Delta v_t} = \frac{v_{t+\Delta t} - v}{|v_t - \bar{v}_t|} \tag{2}$$

where $v_{t+\Delta t}$ is the movement speed at time $t + \Delta t$, $V_t$ is the movement speed at time $t$, $\Delta v_t$ is the relative speed at
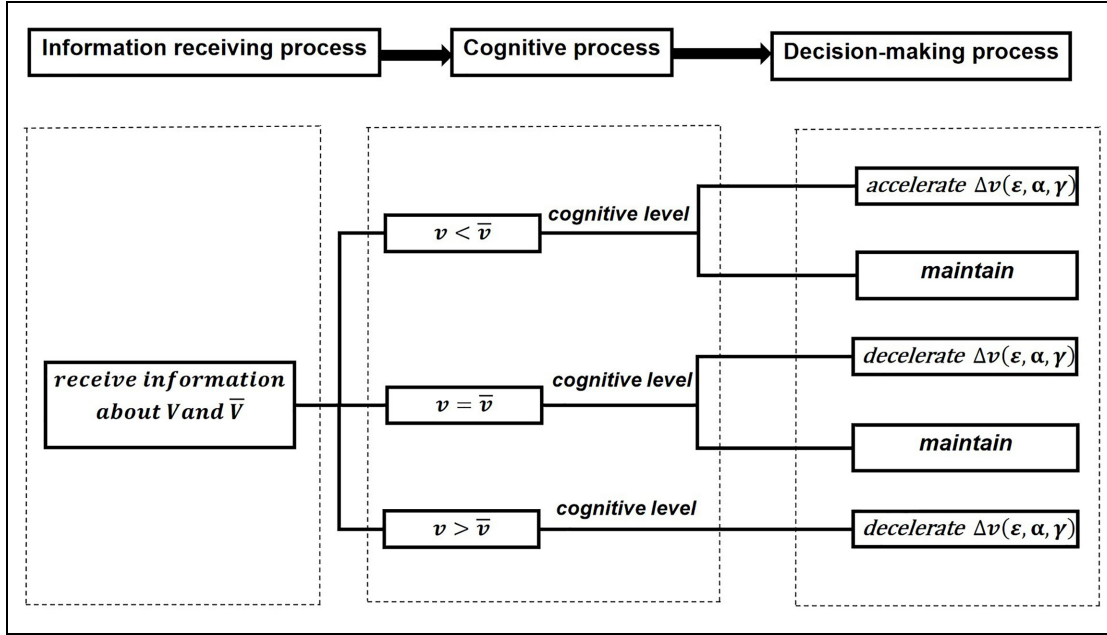
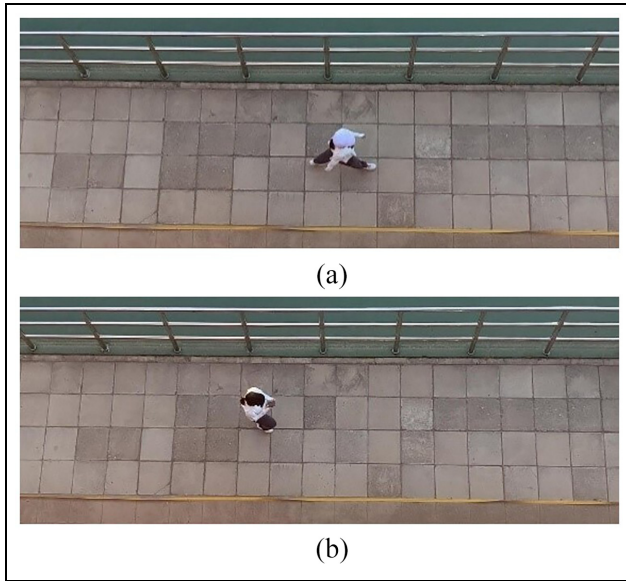**Figure 7.** Pedestrian speed decision-making diagram.



(a)

(b)

**Figure 8.** Speed analysis experiments for (a) VAS and (b) non-VAS pedestrians.



**Figure 9.** Distribution of the VAS deceleration coefficient for pedestrians in a long-distance passage.

speed variation coefficient is calculated for each overtaking behavior. A frequency histogram of the variable speed coefficient is shown in Figure 10 and the corresponding distribution function is shown in Equation (3):

$$f(\alpha) = \frac{1}{0.13\sqrt{2\pi}} e^{\left(-\frac{(\alpha-0.24)^2}{0.0338}\right)} \tag{3}$$

where $f(\alpha)$ is the probability density function of the variable speed coefficient.

### 2.2.3 Slope coefficient.
Experiments were performed to test the effect of ground slope on speed. Considering accidents and uncertainty, it is necessary to assess the effects of human physical strength and endurance on the experimental results. In the experiments, a 10-m-long and 3-m-wide

time $t$, $v_t$ is the relative speed at time $t$, and $\bar{v}_t$ is the speed of influencers at time $t$.

In "Walking direction" section, non-VAS pedestrians were involved in a total of 40 passes of other pedestrians (obvious variable speed behaviors). Therefore, 0.5 s is used as the time interval to calculate the movement speed and the speed variation coefficient $\alpha$ for each pedestrian according to Equation (2). Then, the average value of the
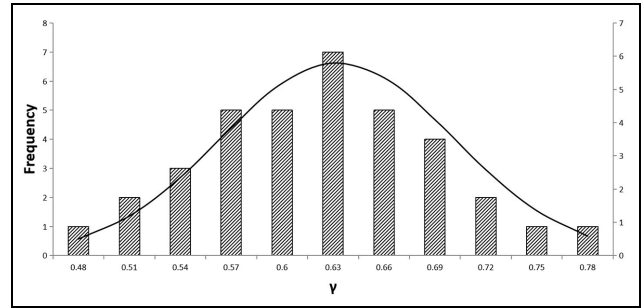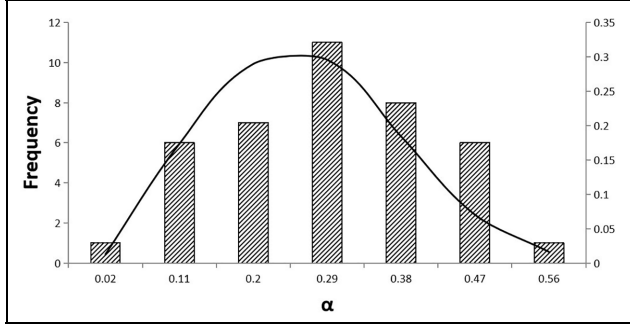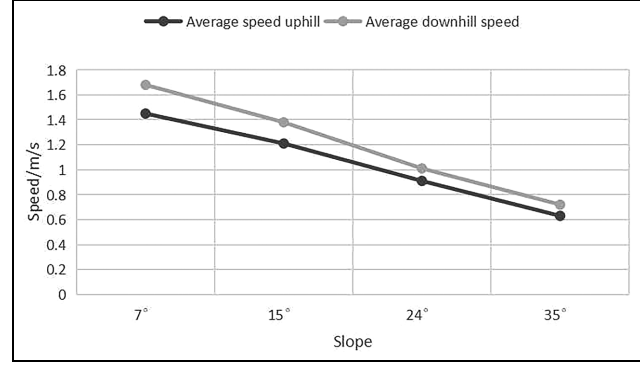
**Figure 10.** Distribution of the non-VAS variable speed coefficient for long-distance passages.



**Figure 11.** Relation between free walking speed and ground slope.

ramp was used. During the experiments, volunteers walked at a chosen walking speed from the starting point to the end point and then returned to the start point after a full rest to complete an experimental cycle. The volunteers were 16 college students, including 8 men and 8 women. In the experiments, four groups were established according to the ground slope; notably, a nearly horizontal ramp (7°), a gently inclined ramp (15°), a moderately inclined ramp (24°), and an inclined ramp (35°) were used. Each experiment was repeated 3 times. The experimental results are shown in Figure 11. After curve fitting, the function relationship between the average speed and the slope when moving up and down a ramp can be obtained, as shown in Equation (4) and Equation (5):

$$v_{up} = -0.276s + 1.74 \qquad (4)$$

$$v_{down} = -0.325s + 2.01 \qquad (5)$$

where $v_{up}$ is the upslope walking speed, $v_{down}$ is the downslope walking speed, and $s$ is the ground slope.

The slope coefficient is the degree of speed reduction caused by slope changes, denoted as $\varepsilon$, and the value range is [0,1]. If $\varepsilon = 0$, the conditions prevent pedestrians from walking; if $\varepsilon = 1$, the conditions do not affect the speed of pedestrians. The corresponding formulas are given in Equation (6) and Equation (7):

$$\varepsilon_{up} = \frac{v_{up}}{v_L} = \frac{(-0.276s + 1.74)}{v_L} \qquad (6)$$

$$\varepsilon_{down} = \frac{v_{down}}{v_L} = \frac{(-0.325s + 2.01)}{v_L} \qquad (7)$$

where $\varepsilon_{up}$ is the upslope coefficient, $\varepsilon_{down}$ is the downslope coefficient, and $v_L$ is the maximum free waking speed of pedestrians in long-distance horizontal passages.

## 3. Model description

In this section, based on the movement characteristics of pedestrians in long-distance passages, a pedestrian flow

evolution equation that considers visual attention using kinetic theory for active particles[29] is proposed. In addition, the relevant variables of the evolution equation, including the interaction rate and transition probability density, are defined.

### 3.1. Kinetic theory for active particles

The kinetic theory for active particles uses the probability distribution of pedestrian states at the microscale to represent the state of the system and a mathematical framework of dynamic changes is derived through balancing the number of pedestrians in the basic domain.[26]

The theory regards pedestrians as active microscopic particles and a pedestrian's microscopic state is represented by time $t$, position $X$, and velocity $V$. In a two-dimensional space, the velocity $V$ is expressed in polar coordinates, that is, $V = \{v, \theta\}$, where $v$ represents the speed and $\theta$ represents the walking direction. Because the units of each variable differ, dimensionless and normalized quantities must be obtained. Time $t$ can be standardized according to the critical time $t_c$ calculated based on the ratio of the characteristic length $l$ to the upper limit speed $v_l$. The components $x$ and $y$ of position $X$ can be standardized based on the characteristic length $l$. Speed $v$ can be standardized based on the upslope speed $v_{up}$ (or downslope speed $v_{down}$).

Because the number of particles can reach millions in kinetic theory, this value can be approximately regarded as the total number of pedestrians moving within the selected velocity range in the established domain. In other words, velocity is represented by a continuous distribution function involving fluid particles. However, the number of people in a passage will be limited and values will fall outside the selected velocity range. Therefore, velocity can be discretized, which is equivalent to a fluid particle only being able to move at certain velocities. Based on this approach, it is assumed that a finite number of pedestrian velocities

are discretized into $p$ speed values and $q$ walking directions and the corresponding discrete sets are given in Equation (8) and Equation (9):

$$I_v = \{v_1 = 0, \ldots, v_j, \ldots v_p = 1\}, \quad j = 1, \ldots, p \quad (8)$$

$$I_\theta = \{\theta_1 = 0, \ldots, \theta_m, \ldots \theta_q = 2\pi\}, \quad l = 1, \ldots, q \quad (9)$$

where $I_v$ is a set of discrete speeds, $I_\theta$ is a set of discrete walking directions, $v_j$ is the $j$ th speed, and $\theta_m$ is the $m$ th walking direction.

Pedestrians are divided into different groups and the number of each group is $i = 1, 2, \ldots, n$; then at time $t$, the microstate of the $i$ th group is described by a probability distribution, as shown in Equation (10):

$$f_i(t, X, V) = f_i(t, X, v, \theta) = \sum_{j=1}^{p} \sum_{l=1}^{q} f_i(t, X)\delta(v - v_j)$$
$$\delta(\theta - \theta_m)$$
$$(10)$$

where $\delta$ is the Dikla function.

Under appropriate integrable conditions, $f_i(t, X, V)dXdV$ represents the number of pedestrians in the elementary domain in the microscopic state $[X, X + dX] \times [V, V + dV]$ at time $t$. The macroscopic variables of the $i$ th group, such as the local density, can be obtained from the weight matrix of the microscopic probability distribution function, as shown in Equation (11):

$$\rho_i(t, X) = \sum_{j=1}^{p} \sum_{l=1}^{q} f_i(t, X) \quad (11)$$

where $\rho_i(t, X)$ is the local density of the $i$ th group and is nondimensionalized based on the maximum density $\rho_{max}$.

To obtain the macrovariables of groups, the sum of variables must be obtained for each group. As an example, the average density can be defined as follows:

$$\rho(t, X) = \sum_{i=1}^{n} \sum_{j=1}^{p} \sum_{l=1}^{q} f_i(t, X) \quad (12)$$

where $\rho(t, X)$ is the average density.

An interaction corresponds to a decision process by which an individual sets their dynamic mechanical state depending on the microstate of the environment and the distribution function of neighboring particles in the interaction domain.[29] Therefore, a mathematical description of the interaction is necessary to establish a mathematical framework for pedestrian movement. In "Motion characteristics of VAS and non-VAS pedestrians in long-distance passages" section, an interaction in a long passage is defined as a decision-making process involving a change in motion state based on the personal cognitive state of an individual after they obtain information about other people and the walls in the interaction domain. The pedestrians involved in an interaction process can be divided into three categories: the affected person before the movement state change, the influencer, and the affected person after the movement state change, which are denoted as $h$, $k$, and $g$, respectively; distribution functions corresponding to these three types of pedestrians are $f_i(t, X, V_*)$, $f_i(t, X, V)$, and $f_i(t, X, V^*)$. Based on the movement characteristics of pedestrians in long-distance passages, an interaction is influenced by the conditions in the objective environment (other pedestrian motion states and the passage walls in the interaction domain) and a pedestrian's subjective initiative is jointly considered. Generally, the environment where the pedestrian is located is objective in a specific case and the subjective initiative of the person influences the degree of the change in their motion state. That is, in a given objective environment, the change in a pedestrian's motion state is random. The transition probability density represents the random dynamic characteristics of the microscopic pedestrian state in a long-distance passage.[29] In addition, because the sight of the affected person may be blocked by external factors, the affected person may not interact with everyone in the interaction domain. This phenomenon can be described by the interaction rate. Hence, this article uses the transition probability density and the interaction rate to describe interactions, and the specific definitions of interactions are the same as those used in previous studies.[25,29]

*Definition 3.1.* The interaction domain is related to the visibility domain and sensitivity domain, and can be defined as a sector with radius $R$ and angle $\Theta$, denoted as $\Omega$.

*Definition 3.2.* The interaction rate is the frequency of interaction between pedestrian $h$ and pedestrian $k$ in the interaction domain in a long-distance passage, which is denoted as $\eta_{hk}[f](X, V_*, V)$.

*Definition 3.3.* Transition probability density is the probability density of pedestrian $h$ and pedestrian $k$, who will become pedestrian $g$ after an interaction in a long-distance passage, denoted as $\mathcal{A}_{hk}[f](V_* \rightarrow V^*|V)$.

The transition probability density for any pedestrian must satisfy Equation (13); specifically, the total transition probability density for the movement state of any pedestrian after all possible changes occur in a given objective environment is equal 1:

$$\int \mathcal{A}_{hk}[f](V_* \rightarrow V^*|V)dV = 1 \quad (13)$$

The relationships among the above variables are summarized in Figure 12.
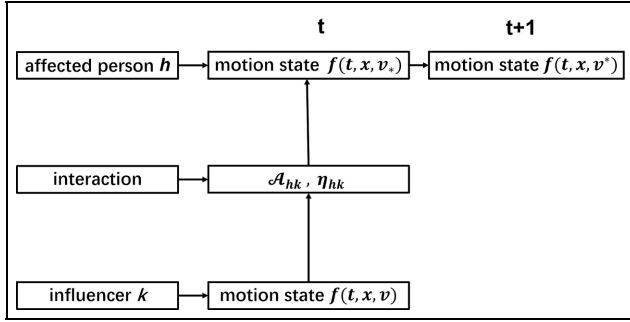
**Figure 12.** Relationship diagram for interaction variables.

Kinetic theory for active particles follows the law of conservation of mass and can be used to derive a continuum equation that describes the state of fluid motion.[29] Similarly, pedestrian dynamics at the mesoscale are associated with the conservation of the number of pedestrians and a mathematical framework[29] for describing the movement of pedestrian flows can be established. The mathematical framework is shown in Equation (14):

$$(\partial_t + V \cdot \partial_x)f_i(t,X,V) = \sum_{k=1}^{n} \int \eta_{ik}$$
$$[f](X,V_*,V)\mathcal{A}_{ik}[f](V_* \to V^*|V)$$
$$\times f_i(t,X,V_*)f_k(t,X,V)dV_*dV$$
$$- f_i(t,X,V^*)\sum_{k=1}^{n}\int \eta_{ik}[f](X,V^*,V)(t,X,V)dV \tag{14}$$

### 3.2. The evolution equation considering visual attention

The abovementioned mathematical framework is a general structure describing the dynamic changes in pedestrian movement in long-distance passages. Visual attention is introduced as a characteristic of pedestrian movement to solve the problem of congestion. A crowd is divided into two groups: non-VAS pedestrians ($i = 1$) and VAS pedestrians ($i = 2$). The probability distribution of each group is shown in Equation (15) and Equation (16):

$$f_1(t,X,V) = f_1(t,X,v,\theta), \quad X \in \sigma, \quad v \in [0,1],$$
$$\theta \in [-45°, 45°] \tag{15}$$

$$f_2(t,X,V) = f_2(t,X,v,\theta), \quad X \in \sigma, \quad v \in [0,1],$$
$$\theta \in [-15°, 15°] \tag{16}$$

Multiple interaction types occur because of the randomness of the walking strategy and they can be divided into two situations: same-group interactions and different-group interactions. Thus, four types of interactions can occur for the two groups, as shown in Table 1.

Based on the interaction types summarized in Table 1, the evolution Equation (17) used to describe the movement of pedestrian flows in long-distance passages can be derived from Equation (15) and Equation (16):

$$(\partial_t + V \cdot \partial_x)f_i(t,X,V) = \sum_{k=1}^{2}\int \eta_{ik}[f](X,V_*,V)$$
$$\mathcal{A}_{ik}[f](V_* \to V^*|V)$$
$$\times f_i(t,X,V_*)f_k(t,X,V)dV_*dV - f_i(t,X,V^*)$$
$$\sum_{k=1}^{2}\int \eta_{ik}[f](X,V^*,V)(t,X,V)dV \tag{17}$$

### 3.3. Modeling interaction rate

The interaction rate is related to the relative speed of the two types of pedestrians in the interaction domain[42] and is given in Equation (18):

$$\eta[f] = \eta_0|V_* - V| \tag{18}$$

where $\eta_0$ is a constant.

The interaction rate is related to not only relative speed but also visibility. Therefore, the visibility of pedestrians is considered when constructing the mathematical expression of the interaction rate, which is given as follows:

$$\eta[f] = \tau\eta_0|V_* - V| \tag{19}$$

where $\tau$ is a coefficient related to visibility and the value range is [0,1].

**Table 1.** Interaction classification table.

| Affected person $h$ | Influencer $k$ | Interaction classification |
| --- | --- | --- |
| Non-VAS pedestrians | non-VAS pedestrians | $1 - 1$ |
| VAS pedestrians | VAS pedestrians | $2 - 2$ |
| Non-VAS pedestrians | VAS pedestrians | $1 - 2$ |
| VAS pedestrians | non-VAS pedestrians | $2 - 1$ |

VAS: visual attention-shifting pedestrians.

## 3.4. Modeling the transition probability density

To construct the formula for the transition probability density, qualitative assumptions are made regarding micro-scale motion phenomena and then they are transformed into mathematical models. The following assumptions are made based on the information presented in "Motion characteristics of VAS and non-VAS pedestrians in long-distance passages" section.

**Assumption 1.** Interactions change the movement state of pedestrians, including their walking direction and speed.

**Assumption 2.** The walking direction of a VAS pedestrian is affected by the destination and the walking direction of a non-VAS pedestrian is affected by the destination, the walls of the movement domain, and the minimum density gradient.

**Assumption 3.** To adapt to the environment of a new position after moving, pedestrians will adjust their speed according to the local speed. If the local speed is higher than their original speed, a pedestrian will increase their speed or maintain their original speed; if the local speed is equal to their original speed, the pedestrian will reduce their speed or maintain their original speed; and if the local speed is lower than their original speed, the pedestrian will reduce their speed.

An interaction is a process in which mobile pedestrians make decisions in a certain order.[29] Based on the information in "Motion characteristics of VAS and non-VAS pedestrians in long-distance passages" section, it is assumed that each pedestrian makes decisions in the following order: (1) the choice of walking direction and (2) speed adjustment. Factoring the speed transition probability density into the functions for the walking direction transition probability density and the speed transition probability density can simplify the expression of the interactions among pedestrians; this expression is given in Equation (20). It is worth noting that Equation (20) is a conceptual model, not a mathematical relationship:

$$\mathcal{A}[f](V_* \to V) = \mathcal{A}^{\theta}[f](\theta_* \to \theta) \times \mathcal{A}^{v}[f](v_* \to v) \quad (20)$$

where $\mathcal{A}$ is the transition probability density of pedestrians, $\mathcal{A}_{\theta}$ is the transition probability density in the walking direction, and $\mathcal{A}_v$ is the speed transition probability density.

### 3.4.1. Modeling the transition probability density in the walking direction. The speed-direction vector for non-VAS pedestrians mainly depends on the exit $V_t$ and the minimum density gradient $V_s$, and the weight of each factor is determined by the transition probability density, which is calculated as follows:

$$V_1'(\cos\theta'_1, \sin\theta'_1) = \frac{((1-\rho)V_t + \rho V_s)}{\|(1-\rho)V_t + \rho V_s\|} \quad (21)$$

where $V_1'$ is the direction vector of a non-VAS pedestrian, $\theta'_1$ is the walking direction of the non-VAS pedestrian, and $V_s = -\nabla\rho/\|\nabla\rho\|$.

To consider the effects of passage walls, Equation (21) needs to be revised. When $V_1'$ effectively points to the destination, there is no need to modify $\theta_1$. When $V_1'$ points to the wall, it needs to be appropriately corrected based on the shortest distance $d_w$ between the pedestrian and a boundary. The specific correction formula is shown in Equation (22):

$$V_1(\cos\theta_1, \sin\theta_1) = (1-d)V_1' + d\mathbf{V}_w \quad (22)$$

where $V_1'$ is the direction vector of the non-VAS pedestrian after correction and $\theta_1$ is the speed-direction vector of the non-VAS pedestrian after correction.

A VAS pedestrian generally chooses to move in the direction of the destination $V_t$; that is, density has little effect on their choices. Therefore, assuming $V_s \cong 0$ for a VAS pedestrian, their walking direction is expressed as shown in Equation (23):

$$V_2(\cos\theta_2, \sin\theta_2) = \frac{V_t}{\|V_t\|} \quad (23)$$

where $V_2$ is the direction vector of the VAS pedestrian and $\theta_2$ is the walking direction of the VAS pedestrian.

Accordingly, the walking direction transition probability density function is given in Equation (24):

$$\mathcal{A}^{\theta}[f](\theta_* \to \theta) = \delta(\theta - \theta_*) \quad (24)$$

### 3.4.2. Modeling the speed transition probability density. According to the information in "Motion characteristics of VAS and non-VAS pedestrians in long-distance passages" section and Assumption 3, pedestrian speed based on the different relationships between $v_*$ and $\bar{v}$ depends on the VAS deceleration coefficient, relative speed, variable speed coefficient, and slope coefficient. The formula for a non-VAS pedestrian can be established as follows:
If $v_* < \bar{v}$:

$$v_1^a = v_* + \alpha\varepsilon(\bar{v} - v_*) \quad (25)$$

$$v_1^b = v_* \quad (26)$$

If $v_* = \bar{v}$:

$$v_1^c = v_* \quad (27)$$

$$v_1^d = \alpha\varepsilon v_* \quad (28)$$

**Table 2.** Speed transition probability density for different interaction types.

| Interaction type | Condition | Speed transition probability density |
|---|---|---|
| I − I | $v_* < \bar{v}$ | $\mathcal{A}^v_{11}[f](v_* \to v) = p_1^a \delta(v_1 - v_1^a) + p_1^b \delta(v_1 - v_1^b)$ |
| | $v_* = \bar{v}$ | $\mathcal{A}^v_{11}[f](v_* \to v) = p_1^c \delta(v_1 - v_1^c) + p_1^d \delta(v_1 - v_1^d)$ |
| | $v_* > \bar{v}$ | $\mathcal{A}^v_{11}[f](v_* \to v) = \delta(v_1 - v_1^e)$ |
| 2 − 2 | $v_* < \bar{v}$ | $\mathcal{A}^v_{22}[f](v_* \to v) = p_2^a \delta(v_2 - v_2^a) + p_2^b \delta(v_2 - v_2^b)$ |
| | $v_* = \bar{v}$ | $\mathcal{A}^v_{22}[f](v_* \to v) = p_2^c \delta(v_2 - v_2^c) + p_2^d \delta(v_2 - v_2^d)$ |
| | $v_* > \bar{v}$ | $\mathcal{A}^v_{22}[f](v_* \to v) = \delta(v_2 - v_2^e)$ |
| 1 − 2 | $v_* < \bar{v}$ | $\mathcal{A}^v_{12}[f](v_* \to v) = p_1^a \delta(v_1 - v_1^a) + p_1^b \delta(v_1 - v_1^b)$ |
| | $v_* < \bar{v}$ | $\mathcal{A}^v_{12}[f](v_* \to v) = p_1^c \delta(v_1 - v_1^c) + p_1^d \delta(v_1 - v_1^d)$ |
| | $v_* > \bar{v}$ | $\mathcal{A}^v_{12}[f](v_* \to v) = \delta(v_1 - v_1^e)$ |
| 2 − 1 | $v_* < \bar{v}$ | $\mathcal{A}^v_{21}[f](v_* \to v) = p_2^a \delta(v_2 - v_2^a) + p_2^b \delta(v_2 - v_2^b)$ |
| | $v_* = \bar{v}$ | $\mathcal{A}^v_{21}[f](v_* \to v) = p_2^c \delta(v_2 - v_2^c) + p_2^d \delta(v_2 - v_2^d)$ |
| | $v_* > \bar{v}$ | $\mathcal{A}^v_{21}[f](v_* \to v) = \delta(v_2 - v_2^e)$ |

If $v_* > \bar{v}$:

$$v_1^e = v_* - \alpha\varepsilon(v_* - \bar{v}) \tag{29}$$

where $v_*$ is the original speed of the non-VAS pedestrian; $v_1$ is the new speed of the non-VAS pedestrian; $a$ is the acceleration strategy for pedestrians when $v_* < \bar{v}$; $b$ is the pedestrian's speed preservation strategy when $v_* < \bar{v}$; $c$ is the pedestrian's speed preservation strategy when $v_* = \bar{v}$; $d$ is the pedestrian's speed reduction strategy when $v_* = \bar{v}$; and $e$ is the pedestrian's speed reduction strategy when $0 \leqslant \bar{v} < v_*$.

The subjective intention of nondistracted particles is affected by the average velocity in the interaction domain $\bar{v}$ and the slope coefficient $\varepsilon$. The average speed in the interaction domain $\bar{v}$ represents the local conditions at the macrolevel, thus providing important information for pedestrians regarding how to adjust their speed. When $\bar{v}$ is large, a pedestrian is generally inclined to increase their speed, and vice versa. The larger $\varepsilon$ is, the more likely a pedestrian is to take action, such as increase speed, and vice versa. For a non-VAS pedestrian represented as a particle $h$, the speed transition probability density is expressed by Equations (30)–(32):
If $v_* < \bar{v}$:

$$\mathcal{A}^v_{1k}[f](v_* \to v) = p_1^a \delta(v_1 - v_1^a) + p_1^b \delta(v_1 - v_1^b) \tag{30}$$

where $p_1^a = \alpha\varepsilon\bar{v}$ and $p_1^b = 1 - \alpha\varepsilon\bar{v}$.
If $v_* = \bar{v}$:

$$\mathcal{A}^v_{1k}[f](v_* \to v) = p_1^c \delta(v_1 - v_1^c) + p_1^d \delta(v_1 - v_1^d) \tag{31}$$

where $p_1^c = \alpha\varepsilon\bar{v}$ and $p_1^d = 1 - \alpha\varepsilon\bar{v}$.
If $v_* > \bar{v}$:

$$\mathcal{A}^v_{1k}[f](v_* \to v) = \delta(v_1 - v_1^e) \tag{32}$$

A non-VAS pedestrian is affected by the average speed of other people in the interaction domain and the slope

coefficient. In addition, VAS pedestrians are limited by their behaviors. The impact of this behavior on speed can be described by the VAS deceleration coefficient $\gamma$. Therefore, Equation (33) is used to calculate the new speed of a VAS pedestrian:

$$v_2 = \gamma v_1 \tag{33}$$

where $v_2$ is the new speed of the VAS pedestrian.

The subjective intention of the VAS pedestrian is affected by the average speed $\bar{v}$ in the interaction domain, the slope coefficient $\varepsilon$, and the VAS deceleration coefficient $\gamma$. The greater the VAS deceleration coefficient $\gamma$ is, the more pedestrians are affected by their behavior, and the greater the tendency to enter the deceleration strategy. For a VAS pedestrian represented as a particle $h$, the speed transition probability density is expressed by Equations (34)-(36):
If $v_* < \bar{v}$:

$$\mathcal{A}^v_{2k}[f](v_* \to v) = p_2^a \delta(v_2 - v_2^a) + p_2^b \delta(v_2 - v_2^b) \tag{34}$$

where $p_2^a = \alpha\varepsilon\bar{v}(1 - \gamma)$ and $p_2^b = 1 - \alpha\varepsilon\bar{v}(1 - \gamma)$.
If $v_* = \bar{v}$:

$$\mathcal{A}^v_{2k}[f](v_* \to v) = p_2^c \delta(v_2 - v_2^c) + p_2^d \delta(v_2 - v_2^d) \tag{35}$$

where $p_2^c = \alpha\varepsilon\bar{v}(1 - \gamma)$ and $p_2^d = 1 - \alpha\varepsilon\bar{v}(1 - \gamma)$.
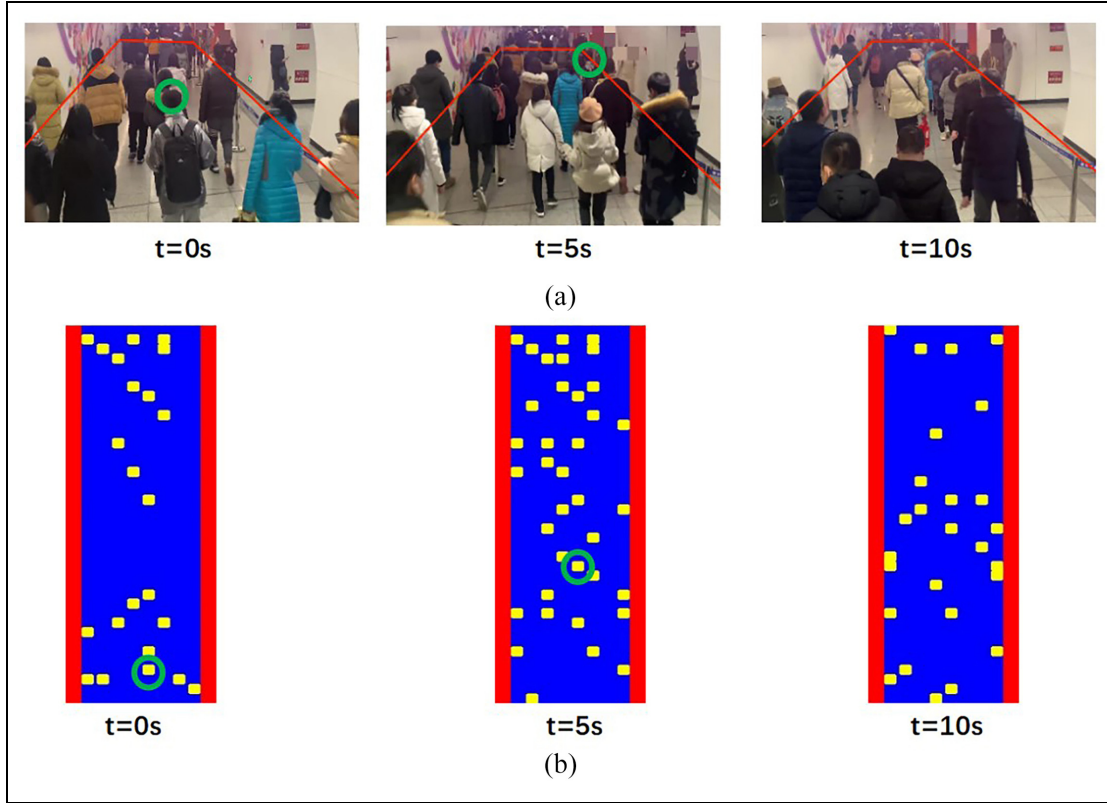If $v_* > \bar{v}$:

$$\mathcal{A}^v_{2k}[f](v_* \to v) = \delta(v_2 - v_2^e) \tag{36}$$

The speed transition probability density $\mathcal{A}^v$ can be summarized as shown in Table 2 for the classification of different interactions.

## 4. Simulations

This section presents some simulations developed to test the predictive ability of the model proposed and shows how to use the model to solve congestion problems

**Figure 13.** Comparisons of (a) real with (b) simulated pedestrian evacuation diagram.

according to ''Model description'' section. The arrangements for this section are as follows: First, we test the validity of the above model, and then, the effect of visual attention shift is displayed; finally, the selection and critical threshold of early warning parameters are shown and discussed.

## 4.1. Validation

The validation of the model was verified by comparing real with simulated pedestrian evacuation diagram for the same subway tunnel in Beijing. We used video cameras on the pedestrian movement of the passage to get real information during the evening rush hour. A 4 m × 12 m channel was taken as the research scene due to the limitation of the shooting picture as shown in Figure 13 and some parts of the image have been specially processed to protect the privacy of pedestrians. The same size channel is built on the simulation platform. The 50th percentile of the maximum shoulder width for Chinese males and females is 0.432 m and 0.351 m, respectively, and the 50th percentile of chest thickness for Chinese males and females is 0.212 m and 0.199 m, respectively.[43] Considering differences in body shape and the computational efficiency of the simulation system, the size of each grid is set to 0.5 m × 0.25 m, and each grid can only

accommodate one pedestrian. Equation (17) is a hyperbolic differential equation. To meet the relevant stability and convergence requirements, the time step should generally not be too large and must meet the Courant, Friedrichs, Lewy (CFL) condition, as shown in Equation (37). Therefore, the minimum value per unit time obtained is 0.1 s from Equation (31):

$$\frac{v\Delta t}{\Delta x} \leqslant C_{max} \qquad (37)$$

where $\Delta t$ is the time step and $\Delta t = 0.1$ s; $\Delta x$ is the characteristic length of the grid, which is 0.25 m or 0.5 m; and $C_{max}$ is the Kurant number, which is 0.7. In addition, the slope coefficient of channel is good, which is good for pedestrians to walk, that is, $\varepsilon = 1$. There are no obstacles that can affect pedestrians' vision, so $\eta_0 = 100\%$. Each pedestrian's initial speed and position is determined by his or her true instantaneous value.

Figure 13 shows that the population distribution of the real scene is roughly the same as that of the model simulation scene above. At $t = 0$ s, the two are the same due to the initial conditions set. When $t = 5$ s, the pedestrian distribution is mostly the same as the actual scene except for one pedestrian marked by the green circle in the figure. The position of the pedestrian is obviously different from

that in the simulation. This is due to the fact that he is looking down at his phone during the initial moments and then he puts it away. In other words, he changed from a VAS pedestrian to a non-VAS pedestrian during walking. However, the model in this paper is based on the assumption that pedestrians do not change their visual attention state during walking, resulting in differences between actual and simulation scenes. In this experiment, a total of 12 VAS pedestrians were found and only one of them had changed visual attention state, which had little influence on the simulation, and this problem should be further considered in the next work to improve the accuracy of the model. At $t = 10$ s, the actual scene and simulated population distribution are roughly the same. In conclusion, the mathematical model can better simulate the crowd movement with visual attention-shifting behavior.

### 4.2. The impact of visual attention shift on congestion

This section selects a subway passage connecting stairs as a simulation scenario because the inconsistent capacity of the subway passage and the connected facilities causes frequent congestion. To simulate pedestrian movement in a subway passage connected to stairs, a 6 m $\times$ 20 m two-dimensional discrete grid system was constructed in the simulation platform. The grid system is composed of a 6 m $\times$ 18 m long straight passage (A) and a 6 m $\times$ 2 m staircase with an exit (B), as shown in Figure 14. The size of each grid is set to 0.5 m $\times$ 0.25 m and each grid can only accommodate one pedestrian. The minimum value per unit time obtained is 0.1 s. In the simulation platform, pedestrians enter the scene randomly and make a one-way movement from the subway transfer channel to the stairs. The proportion of distracted VAS pedestrians is denoted as $\beta$ and the average density in the subway passage is denoted as $\bar{\rho}$. Subway passages and stairs are both types of traffic facilities and it is assumed that stairs are equivalent to subway passages with poor environmental movement conditions. Thus, the movement state changes of pedestrians entering stairwell areas can be simulated using the above model. The speed difference between two pedestrians in a long subway passage and on a stairwell is not large. Therefore, it is assumed that the slope coefficient in area A is relatively, thus promoting walking; that is, $\varepsilon_A = 1$. There is a large difference in pedestrian speed trends for the two visual attention states in area B and we adjust the parameters to $\varepsilon_B = 0.7$ based on the relevant regulations in the "Code for Metro Design."[44] In addition, assuming that there are no obstacles that can affect pedestrian vision, $\eta_0 = 100\%$.

Partial people with visual attention distraction will aggravate the congestion in the crowd, as shown in Figure 15; notably, the images show areas with no visual attention
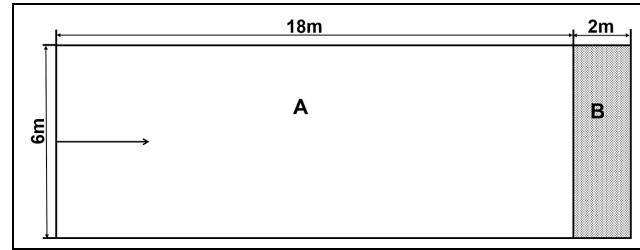


**Figure 14.** Structure diagram of the subway passage connected to stairs. A is the long straight passage. B is the staircase exit.

shifts ($\beta = 0\%$) and some visual attention shifts (assume $\beta = 30\%$) in the population. The former is called the normal population and the latter is called the abnormal population for the convenience of subsequent description. Ten seconds later, there is slight congestion near the exit and the congestion level of the normal population is lower than that of the abnormal population, but the difference is not large in the long corridor. Twenty seconds later, the congestion degree of the normal group does not change significantly, but the congestion level of the abnormal group significantly increases, and the gap between the congestion levels of the two groups increases.

These figures provide evidence of how a shift in visual attention influences the aforementioned patterns and, specifically, induces zones with high-density concentrations that, as is known, can generate congestion. "Motion characteristics of VAS and non-VAS pedestrians in long-distance passages" section shows that the slow behavior of VAS pedestrians will result in overtaking behavior by non-VAS pedestrians. As the number of VAS pedestrians increases, more people will change their evacuation behavior, leading to an increase in group disorder and a slower overall crowd speed, that is, an increased duration of congestion. In actual evacuation scenarios, the congestion risk degree should be controlled to avoid stampedes and other accidents.

### 4.3. Selection and testing of congestion warning parameters

*4.3.1. Selection of congestion warning parameters.* A subway station passage is characterized by multiple facilities in series and thus includes connections involving long-distance passages and stairs. The speed of pedestrians can change significantly at the junctions of facilities. When pedestrians move to facilities with high slope coefficients, their speed will increase. However, when pedestrians move to facilities with low slope coefficients, the crowd speed will decrease. The slope coefficient is positively correlated with shifts in visual attention, as noted in "Motion characteristics of VAS and non-VAS pedestrians in long-distance passages" section; therefore, a speed reduction for a VAS pedestrian will be lower than that for non-VAS
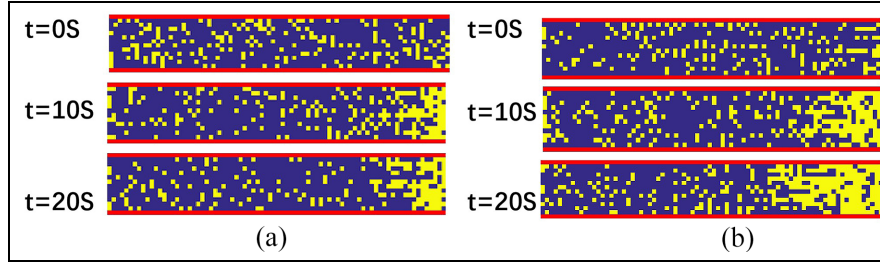
**Figure 15.** Snapshots of evacuation (a) without and (b) with shifts in visual attention.

pedestrians at a junction. Consequently, the greater the proportion of VAS pedestrians is, the more likely that congestion will occur.

In addition, according to shockwave theory,[9] when the pedestrian density is low, the fluctuations caused by a speed reduction will dissipate in a very small area due to the interruption of the pedestrian flow. When the density of pedestrians is high, the fluctuations caused by the deceleration will spread outward and the direction of the fluctuations will be opposite that of pedestrian movement. As pedestrians move forward, new waves will continue to form at junctions. This local disturbance will cause the stability of the system to be unbalanced. In addition, the overall speed in passages will be reduced and queue congestion is prone to occur. Hence, density is related to congestion.

In summary, the density and the proportion of VAS pedestrians, which are denoted as $\beta_{crit}$ and $\bar{\rho}_{crit}$, respectively, are used as congestion warning parameters. Administrators must take measures to prevent the occurrence of congestion if the threshold for one of these parameters is exceeded.

*4.3.2. The critical threshold of $\beta_{crit}$ and $\bar{\rho}_{crit}$.* A numerical definition of congestion is necessary to test $\beta_{crit}$ and $\bar{\rho}_{crit}$. Research shows that when passenger traffic congestion occurs in escalator areas in railway station buildings, pedestrians are more sensitive to queue length than queue time, and queue length expectations can be classified into A-F levels.[45] Therefore, queue length is used as the congestion evaluation standard and the median of grade B (5.63~13.43 people), 10 people (2.5 m), is assumed to be reached; thus, managers need to implement intervention measures.

The critical thresholds for the density and the proportion of VAS pedestrians are tested based on the above standards and the results are presented in Figure 16. Notably, the thresholds are negatively correlated and the slope of the curve exhibits a gradually decreasing trend, which is consistent with the finding that the higher the density of a crowd is, the easier it is for local interference to occur due to shifts in visual attention.[9] Equation (38) is obtained by
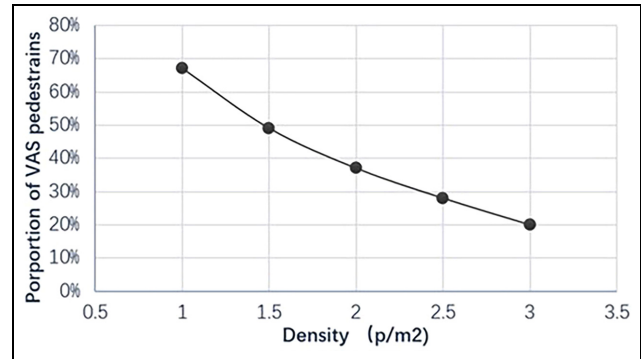


**Figure 16.** The relationship between the proportion of VAS pedestrians $\beta_{crit}$ and the density $\bar{\rho}_{crit}$.

fitting the curve, which can be used as a quantitative basis for preventing congestion.

The results shown in Figure 16 can help managers keep congestion risk within acceptable limits. If a crowd passes through a constrained area, various monitoring technologies[46] can be used to determine the $\beta$ and $\rho$ values in real time. If both variables exceed critical values, namely, $\beta \geqslant \beta_{crit}$ and $\rho \geqslant \bar{\rho}_{crit}$, managers need to implement necessary measures to reduce risk. Specific control measures can be formulated from two perspectives based on reducing the crowd density or the VAS ratio: (1) add safety officers and broadcast announcements to remind pedestrians to change their VAS behaviors, and (2) modify entry points to reduce the number of people entering the passage. The former should be preferred because few measures can be implemented in long subway passages to guarantee the efficiency of crowd movement:

$$\beta_{crit} = 1.2128e^{-0.596\bar{\rho}_{crit}} \tag{38}$$

To intuitively display the changes in the degree of congestion after the corresponding measures are taken, it is assumed that the initial proportion of VAS pedestrians is $\beta = 40\%$ and that when $t = 20$ s, $\beta = 10\%$, which is equivalent to a decrease in the proportion of VAS pedestrians after management measures are implemented, as
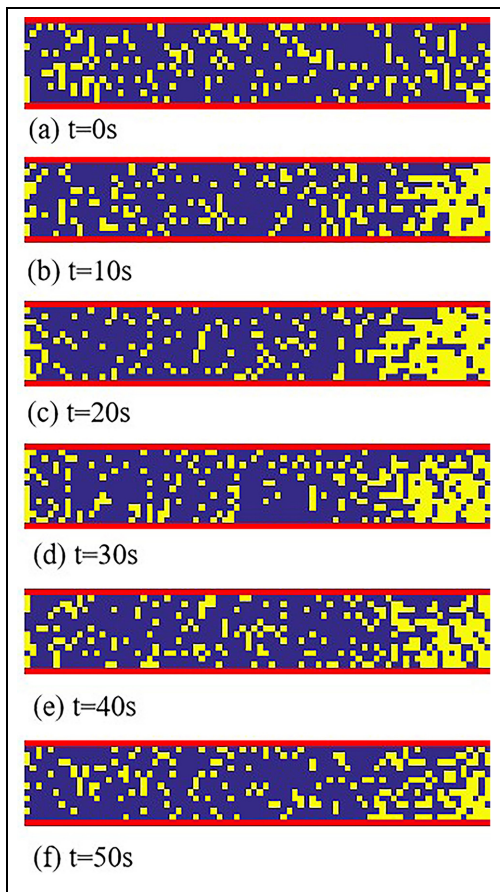
**Figure 17.** Snapshots of an evacuation. The snapshots were obtained at the following times and for the following proportions of VAS pedestrians: (a) $t = 0$ s and $\beta = 40\%$, (b) $t = 10$ s and $\beta = 40\%$, (c) $t = 20$ s and $\beta = 40\%$, (d) $t = 30$ s and $\beta = 10\%$, (e) $t = 40$ s and $\beta = 10\%$, and (f) $t = 50$ s and $\beta = 10\%$.

shown in Figure 17. In the first 20 s, the traffic at the exit worsens over time. After the measures are taken to reduce the proportion of pedestrians with shifts in visual attention, congestion gradually improves. Notably, when the proportion of VAS pedestrians decreases, the congestion level significantly improves. That is, in addition to density, using the VAS ratio as a congestion parameter is valid for managers to deal with evacuation issues.

## 5. Conclusion and future work

In this paper, a kinetic theory model of human crowd movement accounting for visual attention is proposed to solve the problem of congestion in long-distance passages. To provide a realistic basis for the establishment of the model, the proposed motion characteristics of VAS and non-VAS pedestrians are assessed based on investigations and analyses of movement in subway passages. The crowd density and the proportion of VAS pedestrians are selected as early warning parameters that can be used by managers to prevent congestion before a critical threshold is reached. The model is finally used to simulate crowd behaviors in a subway passage connected to stairs. We obtained the following conclusions: (1) The movement characteristics between VAS pedestrians and non-VAS pedestrians are different in practical cases; (2) the simulation results suggest that visual attention has an important impact on congestion; and (3) using the crowd density and the proportion of VAS pedestrians as early warning indicators is effective for preventing the occurrence of congestion, and the critical thresholds of these parameters are negatively correlated.

This model highlights the need to consider visual attention factors in assessments of crowd dynamics and the tested critical values of congestion provide a scientific basis for actual management. Some studies have suggested that emotions have an impact on pedestrian movement.[26,47] People in high-density areas are prone to become irritable and display other emotions, and congestion may involve pushing and other actions in long passages. In addition, the mid-course change of visual attention state mentioned in the validation section should also be taken into account in the mathematical model. Therefore, in future work, the emotions of pedestrians and changes in visual attention state will be considered in the kinetic theory model of human crowds to improve the modeling accuracy.

### ORCID iD

Meiling Wang  https://orcid.org/0000-0001-8605-2706

### References

1. Stutts JC, Reinfurt DW, Staplin LW, et al. The role of driver distraction in traffic crashes. *Distraction*, 2001, https://trid.trb.org/view/690367#:~:text=Distraction%20is%20one%20form%20of,some%20form%20of%20driver%20inattention).
2. Hao Y, Zhang B, Shao C, et al. Exit selection strategy in pedestrian evacuation simulation with multi-exits. *Chinese Phys B: English Vers* 2014; 23: 050512.
3. Zhu KJ and Yang LZ. The effects of exit position and internal layout of classroom on evacuation efficiency. *Acta Phys Sin— Chin Ed* 2010; 59: 7701–7707.
4. Hesham O and Wainer G. Advanced models for centroidal particle dynamics: short-range collision avoidance in dense crowds. *Simulation* 2021; 97: 529–543.

5. Xie CZ, Tang TQ, Zhang BT, et al. Experiment, model, and simulation of the pedestrian flow around a training school classroom during the after-class period. *Simulation* 2022; 98: 63–82.

6. Hao Y, Guan H, Shao C, et al. Simulation of pedestrian evacuation with asymmetrical exits layout. *Physica A* 2011; 390: 198–207.

7. Henein CM and White T. Macroscopic effects of microscopic forces between agents in crowd models. *Physica A* 2007; 373: 694–712.

8. Zhao Y, Liu D and Wang J. Study on the impact of pedestrian using mobile phone on traffic safety in Beijing. *J People's Pub Sec Univers China: Nat Sci Ed* 2015; 2015: 5.

9. Zhang XL, Weng WG and Yuan HY. Empirical study of crowd behavior during a real mass event. *J Stat Mech: Theory E* 2012; 8: P08012.

10. Lewin K. Field theory in social science. *Am Cath Soc Rev* 1951; 12: 103.

11. Helbing D and Molnar P. Social force model for pedestrian dynamics. *Physreve* 1995; 51: 4282.

12. Blue VJ and Adler JL. Cellular automata microsimulation for modeling bi-directional pedestrian walkways. *Transport Res B: Meth* 2001; 35: 293–312.

13. Yi J, Pan S and Chen Q. Simulation of pedestrian evacuation in stampedes based on a cellular automaton model. *Simul Model Pract Th* 2020; 104: 102147.

14. Qin X, Liu H, Zhang H, et al. A collective motion model based on two-layer relationship mechanism for bi-direction pedestrian flow simulation. *Simul Model Pract Th* 2018; 84: 268–285.

15. Zheng Y, Li XG, Jia B, et al. Simulation of pedestrians' evacuation dynamics with underground flood spreading based on cellular automaton. *Simul Model Pract Th* 2019; 94: 149–161.

16. Liu B, Liu H, Zhang H, et al. A social force evacuation model driven by video data. *Simul Model Pract Th* 2018; 84: 190–203.

17. Hughes RL. The flow of large crowds of pedestrians. *Math Comput Simulat* 2000; 53: 367–370.

18. Hughes RL. A continuum theory for the flow of pedestrians. *Transport Res B: Meth* 2002; 36: 507–535.

19. Camilli F, Festa A and Tozza S. A discrete Hughes' model for pedestrian flow on graphs. *Netw Heterog Media* 2016; 12: 93–112.

20. Francesco M, Markowich PA, Pietschmann JF, et al. On the Hughes' model for pedestrian flow: the one-dimensional case. *J Differ Equations* 2011; 250: 1334–1362.

21. El-Khatib N, Goatin P and Rosini M. On entropy weak solutions of Hughes' model for pedestrian motion. *Z Angew Math Phy* 2014; 65: 1289.

22. Amadori DM and Di F. The one-dimensional Hughes model for pedestrian flow: Riemann-type solutions dedicated to Professor Constantine M. Dafermos on the occasion of his 70th birthday. *J Math Phys: Ser B English Ed* 2012; 32: 259–280.

23. Xie J, Chen K, Kwan TH, et al. Numerical simulation of the fire emergency evacuation for a metro platform accident. *Simulation* 2021; 97: 19–32.

24. Bellomo N, Bellouquid A and Knopoff D. From the microscale to collective crowd dynamics. *SIAM J Multiscale Model Simul* 2013; 11: 943–963.

25. Bellomo N and Gibelli L. Toward a mathematical theory of behavioral-social dynamics for pedestrian crowds. *Math Mod Meth Appl S* 2015; 25: 2417–2437.

26. Bellomo N, Gibelli L and Outada N. On the interplay between behavioral dynamics and social interactions in human crowds. *Kinet Relat Mod* 2019; 12: 397–409.

27. Elaiw A and Al-Turki Y. Particle methods simulations by kinetic theory models of human crowds accounting for stress conditions. *Symmetry* 2019; 12: 14.

28. Bellomo N and Bellouquid A. On multiscale models of Pedestrian crowds from mesoscopic to macroscopic. *Comm Math Sci* 2015; 13: 1649–1664.

29. Bellomo N, Burini D, Dosi G, et al. What is life? A perspective of the mathematical kinetic theory of active particles. *Math Mod Meth Appl S* 2021; 31: 1821–1866.

30. Rangel-Huerta A and Muñoz-Meléndez A. Kinetic theory of situated agents applied to pedestrian flow in a corridor. *Physica A* 2010; 389: 1077–1089.

31. Sun Y. Simulations of bi-direction pedestrian flow using kinetic Monte Carlo methods. *Physica A* 2019; 524: 519–531.

32. Bellomo N, Clarke D, Gibelli L, et al. Human behaviours in evacuation crowd dynamics: from modelling to "big data" toward crisis management. *Phys Life Rev* 2016; 18: 1–21.

33. Bellomo N and Gibelli L. Behavioral crowds: modeling and Monte Carlo simulations toward validation. *Comput Fluids* 2016; 141: 13–21.

34. Zhang SX, Shi-Jun LI, Wei YU, et al. Prediction on hot region of crowd abnormal gathering on unexpected event. *China Safe Sci J* 2015; 25: 159–164.

35. Bai L, Wu C, Xie F, et al. Crowd density detection method based on crowd gathering mode and multi-column convolutional neural network. *Image Vision Comput* 2020; 105: 104084.

36. Teo Y, Viswanathan V, Lees M, et al. *Analysing the effectiveness of wearable wireless sensors in controlling crowd disasters*. Elsevier, 2014, https://pure.uva.nl/ws/files/2343394/162760_Analysing_the_Effectiveness_of_Wearable_Wireless_Sensors.pdf

37. Regan Lee MA and Young JD. *Driver distraction: theory, effects and mitigation*. Boca Raton, FL: CRC Press, 2008.

38. Young K, Regan M and Hammer M. Driver distraction: a review of the literature. *Distracted Driving Sydney* 2007; 46: 4266–4269.

39. Ranney TA, Garrott WR and Goodman MJ (eds). *NHTSA driver distraction research: past, present, and future*, 2001, https://www.sae.org/publications/technical-papers/content/2001-06-0177/

40. Daamen W and Hoogendoorn SP. Pedestrian free speed behavior in crossing flows. In: *Traffic and granular flow' 05*, 2007, https://link.springer.com/chapter/10.1007/978-3-540-47641-2_25

41. Aghabayk K, Parishad N and Shiwakoti N. Investigation on the impact of walkways slope and pedestrians physical characteristics on pedestrians normal walking and jogging speeds. *Safety Sci* 2021; 133: 105012.

42. Bellomo N. *Modeling complex living systems*, 2008, https://link.springer.com/book/10.1007/978-0-8176-4600-4
43. Supervision TSBoQaT. *Human dimensions of Chinese adults*. Beijing, China: Standards Press of China, 1988.
44. *The code for design of met*. Beijing, China: China Architecture & Building Press, 2013.
45. He J. *Study on evaluation model of Passenger Traffic Congestion level in urban rail Station*. Beijing, China: Beijing Jiaotong University, 2014.
46. Liu J, Liu W, Wu C, et al. Pedestrian detection method using local feature based on vision attention. *J Image Graph* 2012; 03: 370–379.
47. Cornes FE, Frank GA and Dorso CO. Fear propagation and the evacuation dynamics. *Simul Model Pract Th* 2019; 95: 112–133.

**Author biographies**

**Jun Ma** is a Professor in School of Management and Engineering, Capital University of Economics and Business, China.

**Meiling Wang** is a PhD candidate in School of Management and Engineering, Capital University of Economics and Business, China.

**Linze Li** is a PhD candidate in School of Management and Engineering, Capital University of Economics and Business, China.